



T-Box Transcription Factor 22 Is an Immune Microenvironment-Related Biomarker Associated With the *BRAF*^{V600E} Mutation in Papillary Thyroid Carcinoma

Xubin Dong^{1†}, Jingjing Song^{2†}, Jing Hu^{3†}, Cheng Zheng¹, Xiaohua Zhang^{1*} and Haiguang Liu^{1*}

OPEN ACCESS

Edited by:

Sergio Giannattasio,
Consiglio Nazionale delle Ricerche,
Istituto di Biomembrane,
Bioenergetica e Biotecnologie
Molecolari (IBIOM), Italy

Reviewed by:

Monica Fedele,
Consiglio Nazionale delle Ricerche
(CNR), Italy
Gabriella Guida,
University of Bari Aldo Moro, Italy

*Correspondence:

Xiaohua Zhang
prof.zhang.oncology@gmail.com
Haiguang Liu
liuhgwmu@gmail.com

[†]These authors have contributed
equally to this work and share first
authorship

Specialty section:

This article was submitted to
Molecular and Cellular Oncology,
a section of the journal
Frontiers in Cell and Developmental
Biology

Received: 03 August 2020

Accepted: 24 November 2020

Published: 17 December 2020

Citation:

Dong X, Song J, Hu J, Zheng C,
Zhang X and Liu H (2020) T-Box
Transcription Factor 22 Is an Immune
Microenvironment-Related Biomarker
Associated With the *BRAF*^{V600E}
Mutation in Papillary Thyroid
Carcinoma.
Front. Cell Dev. Biol. 8:590898.
doi: 10.3389/fcell.2020.590898

¹ Department of Thyroid and Breast Surgery, The First Affiliated Hospital of Wenzhou Medical University, Wenzhou, China, ² Department of Children's Health Care, The Second Affiliated Hospital and Yuying Children's Hospital of Wenzhou Medical University, Wenzhou, China, ³ Department of Gastrointestinal Surgery, People's Hospital of Yueqing, Wenzhou, China

Papillary thyroid cancer (PTC) is the most common malignant disease in endocrine systems. T-box transcription factor 22 (TBX22) is a phylogenetically conserved family member that has not been widely characterized in cancers. In this study, we explored the potential clinical significance and biological functions of *TBX22* in PTC. Comprehensive analyses of *TBX22* were based on the public databases and our local qRT-PCR cohort. We observed that *TBX22* was significantly downregulated in PTC compared with normal tissues. *TBX22* was associated with several clinicopathological factors in PTC. Low *TBX22* expression correlated with *BRAF*^{V600E} and TERT mutation. Functional enrichment analysis revealed that cancer-related pathways and immune progress were closely associated with *TBX22* in PTC. In *TBX22*-low PTC, high immune infiltration levels with increased CD8⁺ T cells, natural killer, M1 macrophages, and T-regulatory cells were observed. *TBX22* was negatively correlated with the activity of different steps of the anticancer immunity cycle. Functionally, overexpression of *TBX22* inhibited the proliferation, invasion, and migration in PTC cells, while knocking down of *TBX22* showed the opposite effects. The present findings disclose that *TBX22*, as an immune microenvironment-related biomarker, could be an important tumor suppresser gene and might inform the management of PTC patients better.

Keywords: *TBX22*, papillary thyroid cancer, biomarker, tumor microenvironment, *BRAF*^{V600E}, *RAS*

Abbreviations: PTC, papillary thyroid cancer; *TBX22*, T-box transcription factor 22; BVL, *BRAF*^{V600E}-like; RL, RAS-like; CTLA-4, cytotoxic T lymphocyte-associated antigen 4; TME, tumor microenvironment; TIICs, tumor-infiltrating immune cells; TIME, tumor immune microenvironment; DFI, disease-free interval; PFI, progression-free interval; TMB, tumor mutation burden; MSI, microsatellite instability; GO, Gene Ontology; KEGG, Kyoto Encyclopedia of Genes and Genomes; GSEA, gene set enrichment analysis; TIP, tumor immunophenotype; MAPK, mitogen-activated protein kinase; ssGSEA, single-sample gene set enrichment analysis; PCR, polymerase chain reaction; NC, negative control; CCK-8, Cell Counting Kit-8; OD, optical density; ANOVA, analysis of variance; ROC, receiver-operating characteristic; LNM, lymph node metastasis; VEGFA, vascular endothelial growth factor A; AUC, area under the curve; RSEM, RNA-seq by expectation-maximization; Tc, cytotoxic T cells; Tem, central memory T cells; Tex, exhausted T cells; Tfh, follicular helper T cells; MAIT, mucosal-associated invariant T cells; NK, natural killer cells; MDSC, myeloid-derived suppressor cells.

INTRODUCTION

According to the origin of cells, thyroid cancers are classified into follicular-derived and C-cell-derived. Follicular-derived thyroid cancers are subdivided into anaplastic, papillary (PTC), and follicular thyroid cancers (Landa et al., 2016). Over the past several decades, the rising incidence of PTC has been reported, making it an increasingly important health tissue in most populations of the world (James et al., 2018). Clinical and pathologic factors associated with a somewhat higher risk for PTC recurrence and cancer-related mortality include older age at diagnosis, size of the primary tumor, and the presence of soft-tissue invasion or distant metastases (Johnson et al., 1988; Asioli et al., 2010; Randolph et al., 2012). The prognosis is poorer in patients with specific subtypes of PTC, including tall cell and hobnail variants (Yoo et al., 2016). PTC patients had a favorable overall prognosis, and cancer-specific mortality in non-metastatic PTC patients was only 6% (Ghossein and Livolsi, 2008). However, existing treatments do not sufficiently improve the prognosis of more aggressive and lethal dedifferentiated PTCs.

Papillary thyroid cancer is MAPK-driven cancer with two mutually exclusive drivers, *BRAF*^{V600E} and mutated *RAS*, leading to distinct signaling consequences. Based on this, *BRAF*^{V600E}-like (BVL) and *RAS*-like (RL) are two major PTC molecular subtypes that represent differential regulation of MAPK signaling pathways and thyroid differentiation (Agrawal et al., 2014). RL-PTCs enriched for follicular variant histology result in predominantly well-differentiated tumors, while BVL-PTCs enriched for classical and tall cell histology result in the less differentiated tumor (Ghossein et al., 2007).

The thyroid is the largest endocrine organ in the body and a common target of autoimmune disease. Immune checkpoint blockade like CTLA-4 and PD-1/PD-L1 inhibitors has fueled the field of tumor immunology in thyroid cancer, highlighting both the ability of tumor-immune system treatment and the uniqueness of tumor immunotherapy (Emens et al., 2017). The initiation and progression of the tumor depend on the interaction between the immune system, the TME, and individual tumor cells (Dong et al., 2020a,b). TME is a complex dynamic cell community composed of tumor epithelial cells and a variety of tumor-supporting cells, which represents an important contributor to immortal proliferation, cell invasion, and evasion of immune surveillance (Cheng et al., 2019). Previous studies uncovered that TIICs affect the response rate of immunotherapy, the efficacy of chemotherapy, and the prognosis of patients (Deschoolmeester et al., 2010). There are cancer-promoting and anticancer immune cells within the TIME. The predominance of procancer over anticancer immune cells may be related to cancer progression (Wu et al., 2017). Chen and Mellman (2013) demonstrated the seven steps of the cancer immunity cycle, which have become the basic framework of cancer immunotherapy research. Therefore, it is necessary to evaluate the immune properties of TME to identify the characteristics of novel predictive biomarkers and immune-related molecular in PTC.

T-box is named because this family shares a common DNA-binding domain (Sebé-Pedrós et al., 2013). The T-box genes constitute an ancient family of evolutionarily conserved transcription factors that are crucial to embryonic development by regulating gene expression (Papaioannou, 2014). The T-box gene family was widely studied in the field of developmental biology. Previous studies had demonstrated that mutations in different members of the T-box family result in developmental syndromes, characterized by organ deformity and body structure defects (Miller et al., 2010). In recent years, increasing studies reported that the T-box genes might also function in tumorigenesis and progression in certain cancers (Crawford et al., 2019; Krstic et al., 2019). As a member of the T-box gene family, T-box transcription factor 22 (*TBX22*) mutations caused a high risk of incidence in several diseases, including non-syndromic cleft palate, hypodontia, and ankyloglossia (Braybrook et al., 2001; Kantaputra et al., 2011). However, *TBX22* has so far received little attention in PTC studies.

Recent computational analyses of the RNA-seq profile of bulk tumors allow us to investigate TME in large cohorts. Here, in our study, we comprehensively investigated the expression pattern of *TBX22* and its association with the clinical and pathological parameters of PTC patients. Of note, we evaluated the clinical utility of *TBX22* by correlative analyses with PTC key molecular features, such as *BRAF*^{V600E}, *RAS*, and *TERT* mutation. Based on functional enrichment analysis, we explored the link between *TBX22* and tumor immunity-associated molecular features. Therefore, we performed a series of experiments to demonstrate the effect of overexpression and knocking down *TBX22* on PTC cell lines. Our findings were largely consistent in public cohorts and our local PTC profile.

MATERIALS AND METHODS

Bioinformatics

This study applied multiple public PTC cohorts. For The Cancer Genome Atlas (TCGA) dataset, RNA-seq and clinical profiles of human thyroid cancer patients were obtained from the TCGA data portal (Agrawal et al., 2014). TCGA RNA-seq profile contained 568 samples, comprising 59 matched normal samples, 501 PTC samples, and eight metastatic thyroid carcinoma samples. Whole-transcriptome sequencing data were aligned using RSEM expression level in transcripts per million. The definition and outcome of DFI and PFI were extracted from the TCGA-Clinical Data Resource (Liu et al., 2018). Mutation status was obtained from Mutation Annotation Format files (derived from VarScan2) from the Genomic Data Commons portal. TMB was calculated by the sum of the number of non-silent mutations in the TCGA samples. MSI status (MANTIS score) for the TCGA cohort was obtained from a previous publication (Bonneville et al., 2017). Expressional data and corresponding clinical profiles of GSE33630 (Dom et al., 2012), GSE60542 (Tarabichi et al., 2015), and GSE35570 (Yu et al., 2008; Handkiewicz-Junak et al., 2016) datasets were obtained from the GEO database.

Correlation analysis was assessed by the function “cor.test” in R. Genes which had Spearman correlation value >0.4 or

<-0.4 , $p < 0.001$ with *TBX22* were selected. GO and KEGG analyses were performed using “enrichGo” and “enrichKEGG” functions in the “clusterProfiler” package, respectively. “ggplot2” and “pheatmap” packages were used for visualization. The GSEA was performed using the hallmark collections from the Molecular Signature Database (Subramanian et al., 2005). FDR-adjusted q -value <0.25 was set as the cutoff to identify significantly enriched terms.

The ESTIMATE algorithm was used to quantify the immune and stromal proportions in the PTC microenvironment (Yoshihara et al., 2013). For specific TIIC infiltration analyses, quanTIseq and ImmuCellAI algorithms were used to estimate the relative proportions of immune cell types in TME. ImmuCellAI is a gene-expression-based pipeline for the quantification of the tumor immune contexture from human RNA-seq profiles (Miao et al., 2020). quanTIseq is a deconvolution-based algorithm, providing “absolute score” representing cell fractions in TME (Finotello et al., 2019). The TIP pipeline was applied for cancer immunity cycle profiling (Xu et al., 2018). This method used an algorithm based on ssGSEA to evaluate the relative activity of the seven steps of the immune cycle, which is a process by which the immune system recognizes and kills cancer cells in a large number of tumor samples.

Patients and Thyroid Tissue Samples

Seventy-nine pairs of PTC and corresponding normal thyroid tissues were obtained from the Department of Thyroid and Breast Surgery, The First Affiliated Hospital of Wenzhou Medical University. Furthermore, all surgical specimens were independently confirmed by two experienced pathologists, and the results showed that 79 pairs of surgical specimens all met the diagnosis of PTC and normal thyroid tissues, respectively. The collected fresh tissues were immediately snap-frozen in liquid nitrogen and stored at -80°C until further RNA was detected. *BRAF*^{V600E} mutation detection was performed on the extracted DNA from preoperative fine-needle aspiration cells after cytologic evaluation. Briefly, each real-time PCR mixture contained 5 μl of extracted DNA and other reagents available in the detection kit ADx-Amplification Refractory Mutation System (AmoyDx, China). Clinical and pathological features of patients in the TCGA and WMU-THCA cohorts are presented in Tables 1, 2, respectively.

qRT-PCR

Total RNA was isolated from patient tissue and thyroid cancer cell lines by TRIzol reagent (Invitrogen, United States). All RNA samples were temporarily stored at -80°C . The isolated RNA was measured at 260/280 nm to ensure the reliability of RNA quality and quantity. The range of 260/280 nm is between 1.72 and 1.95. The ReverTra Ace qPCR RT Kit (Toyobo, Japan) was used for RNA reverse transcription. Real-time PCR was run and analyzed using the 7500 Fast quantitative PCR System (Applied Biosystems, United States). The relative expression of *TBX22* mRNA was presented using the method of $2^{-\Delta\Delta CT}$ with the endogenous control *GAPDH* to normalize the data. The primer sequences used were as follows: *TBX22* forward primer, 5'-CCUUUGAACUCCUUACUUUTT-3'; *TBX22* reverse primer,

TABLE 1 | Baseline of patients in the TCGA cohort.

	Level	Overall
<i>n</i>		501
Age (median [IQR])		46.00 [35.00, 58.00]
Race (%)	American Indian or Alaska native	1 (0.2)
	Asian	52 (12.7)
	Black or African American	26 (6.3)
	White	331 (80.7)
Gender (%)	Female	366 (73.1)
	Male	135 (26.9)
Pathologic stage (%)	Stage I	282 (56.5)
	Stage II	51 (10.2)
	Stage III	111 (22.2)
	Stage IV	55 (11.0)
Pathology T stage (%)	T1	141 (28.1)
	T2	166 (33.1)
	T3	169 (33.7)
	T4	23 (4.6)
Pathology N stage (%)	N0	226 (45.1)
	N1	226 (45.1)
Pathology M stage (%)	M0	279 (55.8)
	M1	9 (1.8)
Radiation therapy (%)	No	180 (37.1)
	Yes	305 (62.9)
Histological type (%)	Others, specify	7 (1.4)
	Classical/usual	357 (71.3)
	Follicular	102 (20.4)
	Tall cell	35 (7.0)
Radiation exposure (%)	No	421 (96.1)
	Yes	17 (3.9)
Extrathyroidal extension (%)	Minimal (t3)	133 (27.5)
	Moderate/advanced (t4a)	18 (3.7)
	None	331 (68.5)
	Very advanced (t4b)	1 (0.2)
Residual tumor (%)	R0	383 (81.7)
	R1	52 (11.1)
	R2	4 (0.9)
Multifocality (%)	Multifocal	227 (46.2)
	Unifocal	264 (53.8)

5'-AAAGUAAAGGAGUUCAAAGGTT-3'; *GAPDH* forward primer, 5'-GTCTCCTCTGACTTCAACAGCG-3'; *GAPDH* reverse primer, 5'-ACCACCCTGTTGCTGTAGCCAA-3'.

Cell Cultures and Transient Transfection With Plasmids or siRNAs

BCPAP, TPC-1, and KTC-1 cells were cultured in Roswell Park Memorial Institute 1640 medium (Gibco, United States) supplemented with 10% FBS (PAN Biotech, Germany). DMEM (Gibco, United States) supplemented with 10% FBS was used for growing FTC and HTori-3 cells. These cells were incubated in a humidified incubator at 37°C with 5% CO_2 . Cells used in the present study were all obtained from Shanghai Cell Biology,

Institute of the Chinese Academy of Sciences (Shanghai, China). Employed cell lines have different genotypes, as shown in **Table 3**.

For *TBX22* overexpression, the structure of vectors contained the full length of *TBX22* and was constructed into CMV-MCS-EGFP-SV40-Neomycin. pcDNA3.1-*TBX22* and its empty vector were purchased from GeneChem (Shanghai, China) according to the manufacturer's recommendations. Transient siRNA transfection for *TBX22* was obtained from RiboBio (Guangzhou, China) for cell interference. Based on the manufacturer's protocol, Lipofectamine RNAiMAX transfection reagent (Thermo Fisher Scientific, United States) was mixed with siRNA to transfect cancer cell lines. The negative control (si-NC) was not homologous to any human genomic sequence tracks. The siRNA sequences are listed as follows: si-TBX22: sense: 5'-CCUUUGAACUCCUACUUUTT-3', antisense: 5'-AAAGUAAGGAGUUCAAAGGTT-3'.

Cellular Proliferation, Migration, and Invasion Assay

To determine the ability of cell proliferation, the Cell Counting Kit-8 (CCK-8, Beyotime, China) was employed in this study.

Forty-eight hours after siRNA transfection, 1,500 cells were seeded into each well of a 96-well plate with 100 μ l medium supplemented with 10% FBS. At every indicated time point, the medium was exchanged by 100 μ l medium with CCK-8 (91 μ l medium and 9 μ l CCK-8), and the cells were incubated in 5% CO₂, 37°C for 3 h. The OD at a wavelength of 450 nm in each well was recorded on a microplate reader (SpectraMax Plus 384, Molecular Devices Corporation, CA, United States). For the colony formation assay, about 1,000 transfected cancer cells were added to each well in a six-well plate and incubated for 10–14 days until colonies were formed. The plates were then gently washed with PBS and stained with crystal violet. Colony areas were determined by the ColonyArea plugin (Guzman et al., 2014) in ImageJ software. Transwell plates (Corning, NY, United States) were used for the migration assay. Cells (4×10^4 cells/chamber) were seeded onto the upper chamber, and the growth medium containing 10% FBS was added to the bottom chamber. After 24 h and 37°C incubation, non-migrated cells on the upper chamber were carefully removed with a cotton swab. Cells migrating through the filter chamber were fixed with methanol and stained with 0.1% crystal violet. For the invasion assay, an identical protocol was followed, except that the chamber is Matrigel invasion chamber (Corning Incorporated). Migrated or invaded cells were imaged in a 10 \times magnification microscope in five random fields for each well and quantified by ImageJ software.

Statistical Analysis

Mann–Whitney test or Wilcoxon signed-rank test was used in the two-group analysis. Comparisons between different groups were conducted by Kruskal–Wallis one-way ANOVA. Correlation analyses between two variables were calculated using Spearman Rho. These variables included gene expression levels, TME signature scores, TMB, and MSI scores. The ROC curve analysis estimated the biomarker value of *TBX22*. and the Kaplan–Meier curves and log-rank tests were used to evaluate differences in prognosis. The optimal *TBX22* cutpoints for Kaplan–Meier curves were calculated using the “res.cut” function. Patients with full clinical information were selected for the Cox regression analysis, and we removed patients with a follow-up period of fewer than 30 days. Uni- and multivariable Cox regression models were built using the clinical and pathological parameters along with the respective *TBX22* expression data by the “coxph” function in the “survival” package. R 3.5.2 and GraphPad Prism 8.2.0 were utilized in this study.

TABLE 2 | Baseline of patients in the WMU-THCA cohort.

	Level	Overall
<i>n</i>		79
Age (median [IQR])		43.00 [33.00, 52.00]
Gender (%)	Female	59 (74.7)
	Male	20 (25.3)
Pathology T stage (%)	T1	60 (75.9)
	T2	13 (16.5)
	T3	6 (7.6)
Extrathyroidal extension (%)	None	65 (82.3)
	Yes	14 (17.7)
Pathology N stage (%)	N0	31 (39.2)
	N1	48 (60.8)
<i>BRAF</i> ^{V600E} (%)	Negative	11 (13.9)
	Positive	48 (60.8)
AJCC7 stage (%)	Stage I	30 (38.0)
	Stage II	46 (58.2)
	Stage III	3 (3.8)
Envelop invasion (%)	No	24 (30.3)
	Yes	8 (10.1)
Multifocality (%)	Multifocal	33 (41.8)
	Unifocal	46 (58.2)

TABLE 3 | Genotype of the employed PTC cell lines.

Cell lines	Category	<i>BRAF</i>	<i>NRAS</i>	<i>HRAS</i>	<i>KRAS</i>	<i>TERT</i>	<i>RET/PTC1</i>	Resource
BCPAP	PTC cell lines	GTG- > GAG V600E*	wt	wt	wt	c.1-124C > T (c.228C > T) [†]	wt	Meireles et al., 2007; Landa et al., 2019
TPC-1	PTC cell lines	wt	wt	wt	wt	c.1-124C > T (c.228C > T) [†]	+	Meireles et al., 2007; Landa et al., 2019
KTC-1	PTC cell lines	GTG- > GAG V600E*	wt	wt	wt	c.1-146C > T (c.250C > T) [†]	wt	Landa et al., 2013, 2019

wt, wild-type genotype; +, presence of the gene rearrangement. [†]TERT promoter mutations. *Heterozygous mutation.

RESULTS

The Expression Level of *TBX22* in PTC

For PTC patients (TCGA cohort), *TBX22* was significantly lower in PTC than in the corresponding normal thyroid tissue (Figure 1A, $p < 0.0001$), which was also compatible in the GSE33630, GSE60542, and GSE5364 cohorts (Figures 1B–D, all $p < 0.0001$). To validate the transcription level of *TBX22* in our local PTC patients, we performed qRT-PCR of 79 pairs of tumor samples and adjacent normal thyroid tissues, and *TBX22* was downregulated in PTC tissues compared with that in adjacent normal tissues (Figure 1E, $p < 0.0001$). These results demonstrated that *TBX22* was downregulated in PTC.

The Expression of *TBX22* Was Negatively Correlated With the Development of PTC

Next, we analyzed the relationship between mRNA expression of *TBX22* and the PTC clinicopathological parameters in the TCGA database and the local WMU cohort. In the TCGA cohort, the mRNA level of *TBX22* in PTC patients was significantly associated with tumor size (Figure 2A, $p = 1.6e-05$), nodal metastasis (Figure 2B, $p = 1.9e-06$), extrathyroidal extension (Figure 2C, $p = 7.1e-08$), and disease stage (Figure 2D, $p = 0.003$). In addition, *TBX22* level was significantly higher in the follicular variant subtype compared with the tall cell variant (Figure 2E, $p = 1.6e-05$) and classical subtypes (Figure 2E, $p = 1.3e-09$). Our further analysis of *TBX22* profiles of the local cohort validated that the expression of *TBX22* was significantly associated with tumor size (Figure 2F, $p = 0.012$) and LNM (Figure 2G, $p = 0.0051$). We also observed that *TBX22* had a trend in distinguishing between PTC patients with and without extrathyroidal extension (Figure 2H, $p = 0.11$).

Association Between *TBX22* and Molecular Characteristics

Papillary thyroid cancer can be classified according to 71 gene expression signatures as BVL and RL (Cancer Genome Atlas Research Network, 2014). Thus, we divided patients according to their driver mutation status and found that *TBX22* expression was significantly lower in the *BRAF*^{V600E} (Figure 3A, $p < 0.0001$) and *TERT* mutation groups (Figure 3C, $p = 0.045$). However, the expression of *TBX22* was higher in the *RAS* wild-type group (Figure 3B, $p < 0.0001$) than in their respective counterpart groups. Besides, *TBX22* showed a trend in distinguishing between the *RET* fusion group and the *RET* wild-type group (Figure 3D, $p = 0.059$). *TBX22* expression was significantly lower in the BVL group than in the RL group (Figure 3E, $p < 0.0001$). In addition, *TBX22* showed a strong positive correlation with *VEGFA* (Figure 3F, $R = 0.66$, $p < 0.0001$). However, *TBX22* was weakly correlated with scores of TMB (Figure 3G, $R = -0.11$, $p = 0.016$) and MSI (Figure 3H, $R = -0.1$, $p = 0.028$).

TBX22 Could Serve as a Robust Biomarker in PTC Patients

Based on these results, we hypothesized that *TBX22* could serve as a biomarker for PTC and ROC curve analysis demonstrated

that *TBX22* was diagnostically significant with an AUC value of 0.9343, 0.9504, 0.9704, 0.9407, and 0.9189 in the TCGA, GSE33630, GSE35570, GSE60542, and our validated local cohorts, respectively (Figure 4A). *TBX22* also had predicted value for the T stage in TCGA cohort (AUC = 0.6195) and our local cohort (AUC = 0.6873, Figure 4B). For LNM, the AUC was 0.6289 in TCGA and 0.6683 in our validated cohort (Figure 4C). Importantly, the AUC for distinguishing *BRAF*^{V600E} (mutated vs. wild type) was 0.7135 in TCGA and 0.7536 in our local validated cohort (Figure 4D). Our results suggested that *TBX22* could be exploited as a reliable predictive biomarker for PTC patients.

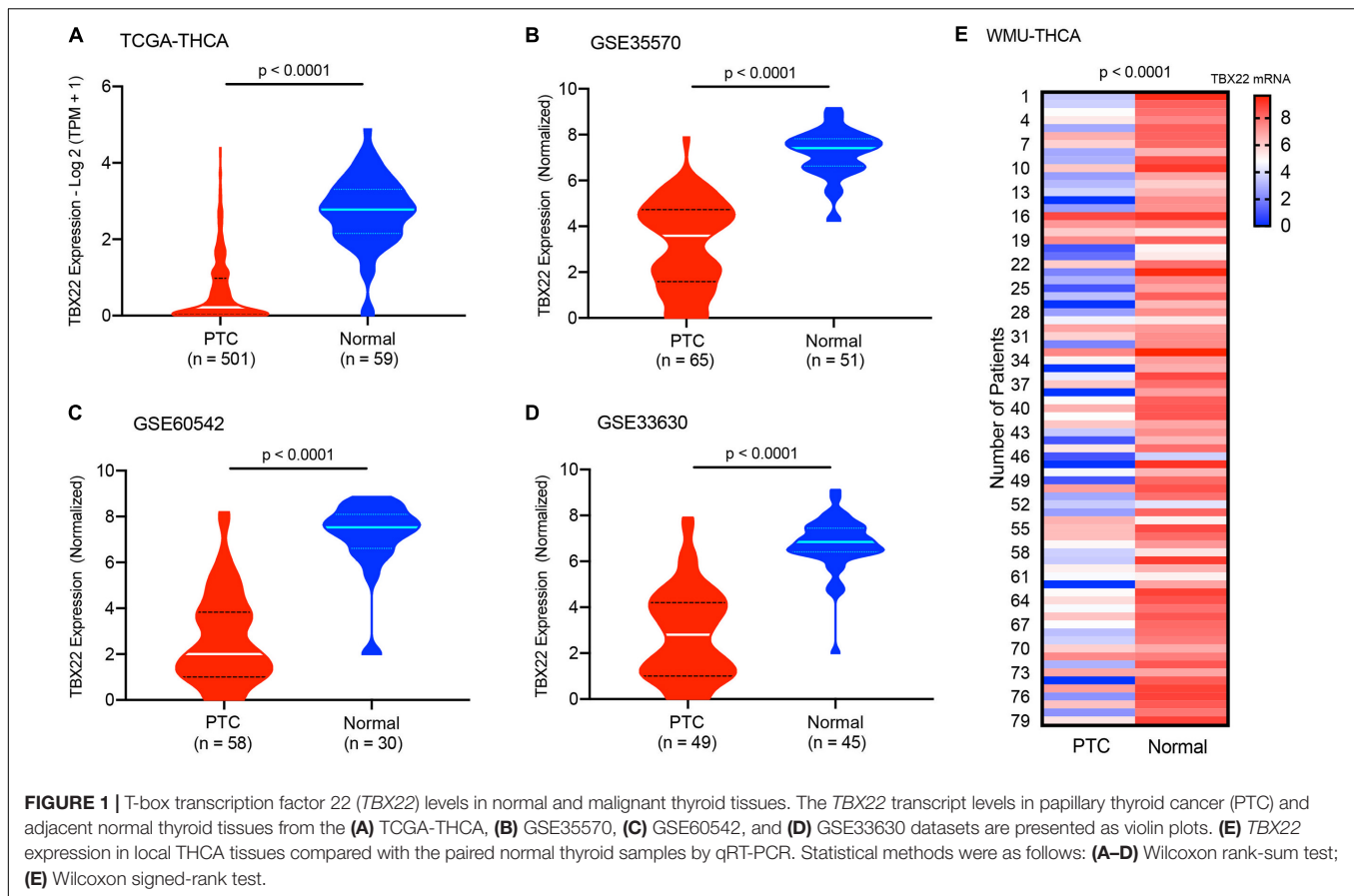
We hypothesized that *TBX22* could be a prognostic biomarker for PTC patients. In the survival analysis, *TBX22* expression alone is significantly associated with better DFI (Figure 4E, HR: 2.05; 95% CI: 1.04–4.56; $p = 0.045$) and PFI (Figure 4F, HR: 1.93; 95% CI: 1.12–3.35; $p = 0.017$) in PTC patients. Using univariate Cox regression analyses, we identified disease stage, T stage, extrathyroidal extension, LNM, and *TBX22* were significantly associated with DFI and PFI (Supplementary Table 1). However, we did not find independent prognostic factors in multivariate Cox regression analyses (Figures 4G,H).

Predicted Functions and Pathways of *TBX22* in PTC

In a specific biological environment, genes interact with each other and drive the underlying pathway and molecular function (Jia et al., 2016). Based on this, we utilized the TCGA dataset to perform co-expression analysis to elucidate the most relevant genes with *TBX22*. We further selected the genes with strong co-expression correlation with *TBX22* (Spearman correlation value >0.4 or <-0.4 , $p < 0.0001$) for GO and KEGG analyses (Figures 5A,B and Supplementary Tables 2–4). GO enrichment and KEGG enrichment analyses unanimously suggested that *TBX22* is prevalently correlated with thyroid hormone metabolism, immune activation, and MAPK signaling pathways. Consistently, GSEA via the hallmarks database revealed that the low *TBX22* subset was prevalently enriched in various tumorigenesis pathways and immune-activating processes (Figure 5C and Supplementary Table 5). These well-reproductive results revealed that *TBX22* might have intrinsic roles in tumor immunity and PTC progression.

TBX22 Expression Correlates With TIICs and Cancer Immunity Cycle in TIME

Previous studies have revealed that TIICs are extensively distributed in TME of PTC and influence the different stages of tumorigenesis and development. Stromal score and immune score represent the percentage of stromal cells and immune cells in the TME, respectively (Mao et al., 2013). *TBX22*^{high} and *TBX22*^{low} groups were divided based on the median value of the *TBX22* expression in the TCGA profiles. We adopted the ESTIMATE algorithm to evaluate the immune microenvironment and stromal microenvironment in the PTC samples. In the *TBX22*^{low} group, the immune score and TME score were higher, whereas tumor purity was lower compared with that in the *TBX22*^{high} group (Figure 6A). However,



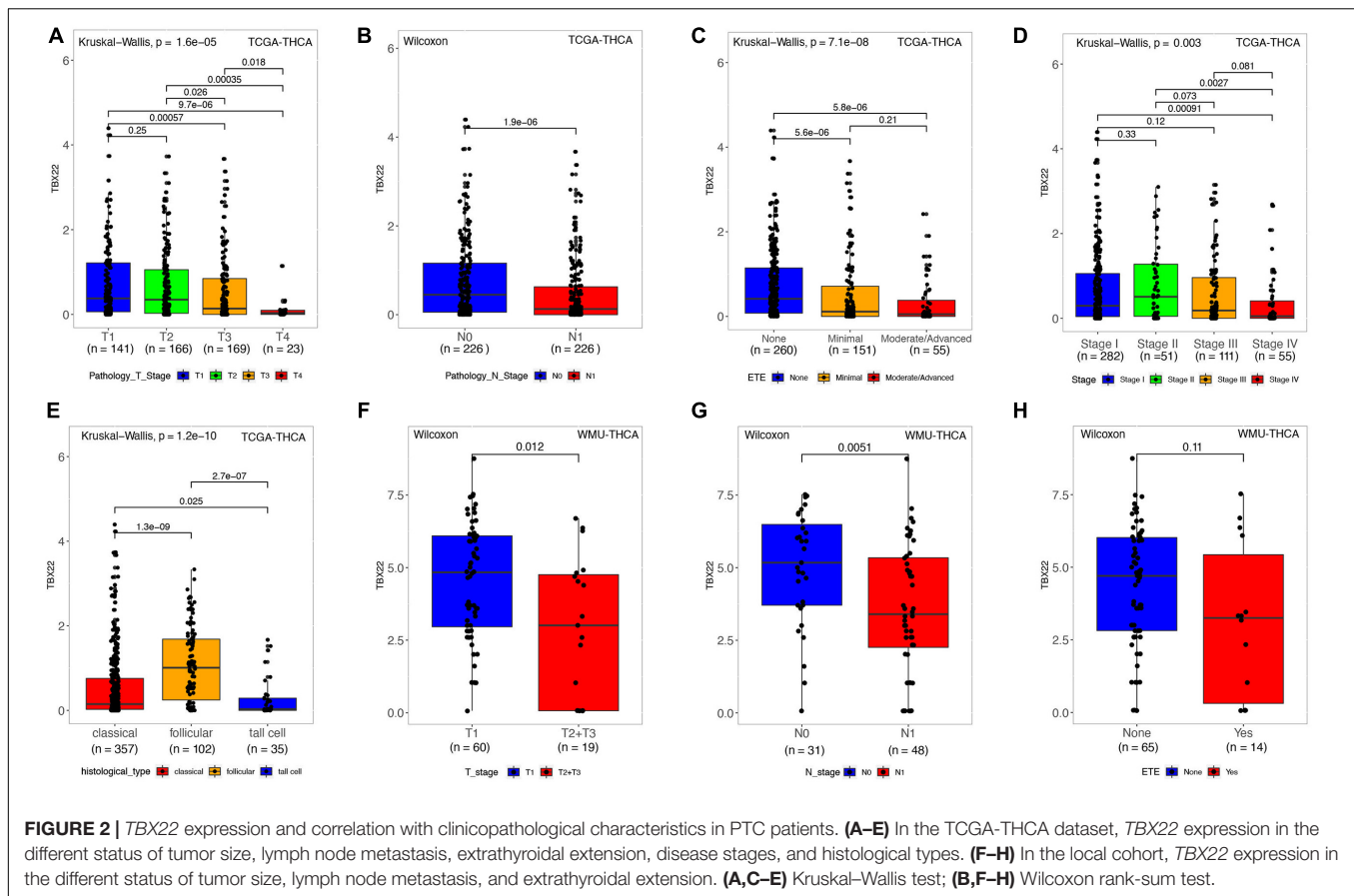
no significant association between stromal scores and *TBX22* expression was found (Figure 6B). In general, these analyses revealed that the expression of *TBX22* was negatively correlated with the immune scores in PTC. To explore the correlation of *TBX22* expression with the immune microenvironment, we inferred the abundance of TIICs by establishing two different algorithms, quantIseq and ImmuCellAI. The landscapes of TIICs and clinical-pathological features are shown in Figures 6C,D. The hierarchical clustering of the whole-sample RNA-seq profile classified immune cells into four subgroups. Moreover, the proportions of TIICs were weakly to highly correlated (Figures 6E,F).

We tried to determine whether the TIME was altered among patients with different levels of *TBX22* (Figures 7A,B). *TBX22*^{low} PTC was associated with significantly higher anticancer M1 macrophages and significantly lower procancer M2 macrophages; anticancer Th1 cells were higher in *TBX22*^{low} PTC, while procancer Th2 cells did not have a significant difference between different *TBX22* states. The levels of anticancer CD8⁺ T cells and procancer regulatory T cells were both elevated in *TBX22*^{low} PTC. At the same time, *TBX22*^{low} PTC had a higher number of anticancer T-follicular helper cells. NK cells did not have a significant difference between different *TBX22* states. Strikingly, CD4⁺ T cells were also lower in the *TBX22*^{low} PTC. ImmuCellAI infiltration score, an assessment of universal immune cytolytic activity, was also higher in the *TBX22*^{low} group (Figure 7B).

The cancer immunity cycle triggers a series of gradual events and enables the anticancer immune response to effectively kill cancer cells (Chen and Mellman, 2013). As shown in Figure 8, after releasing cancer cell antigen and presenting cancer antigen, effector T-cell responses against the cancer-specific antigens were primed and activated (step 1 to step 3). *TBX22*^{low} PTC had higher immune activity in step 3 compared with *TBX22*^{low}. We observed that the *TBX22*^{low} PTC had higher anticancer immunity scores in the trafficking of T cells to tumors (step 4) and infiltration of T cells into tumors (step 5). *TBX22*^{low} PTC had a significantly higher level of recruiting CD8⁺ T cells, Th1, Th22, neutrophil, natural killer, eosinophil, basophil, B cells, Th2, and MDSCs. Interestingly, an elevated level of recognition of cancer cells by T cells (step 6) was observed in *TBX22*^{high} PTC. In summary, *TBX22*^{low} state may be associated with active anticancer immune response, and *TBX22* had a negative role in the cancer immunity cycle.

Dysregulation of *TBX22* Affects Thyroid Cancer Cell Proliferation, Migration, and Invasion

To complement the above bioinformatic analyses, we verified the expression of *TBX22* in PTC cell lines. Compared with the normal thyroid cell lines (HTori-3), the *TBX22* level was significantly lower in PTC cell lines (BCPAP, TPC-1, and KTC-1) (Figure 9A).



Next, we sought to elucidate the functional effects of *TBX22* dysregulation through studies *in vitro* on PTC cell lines.

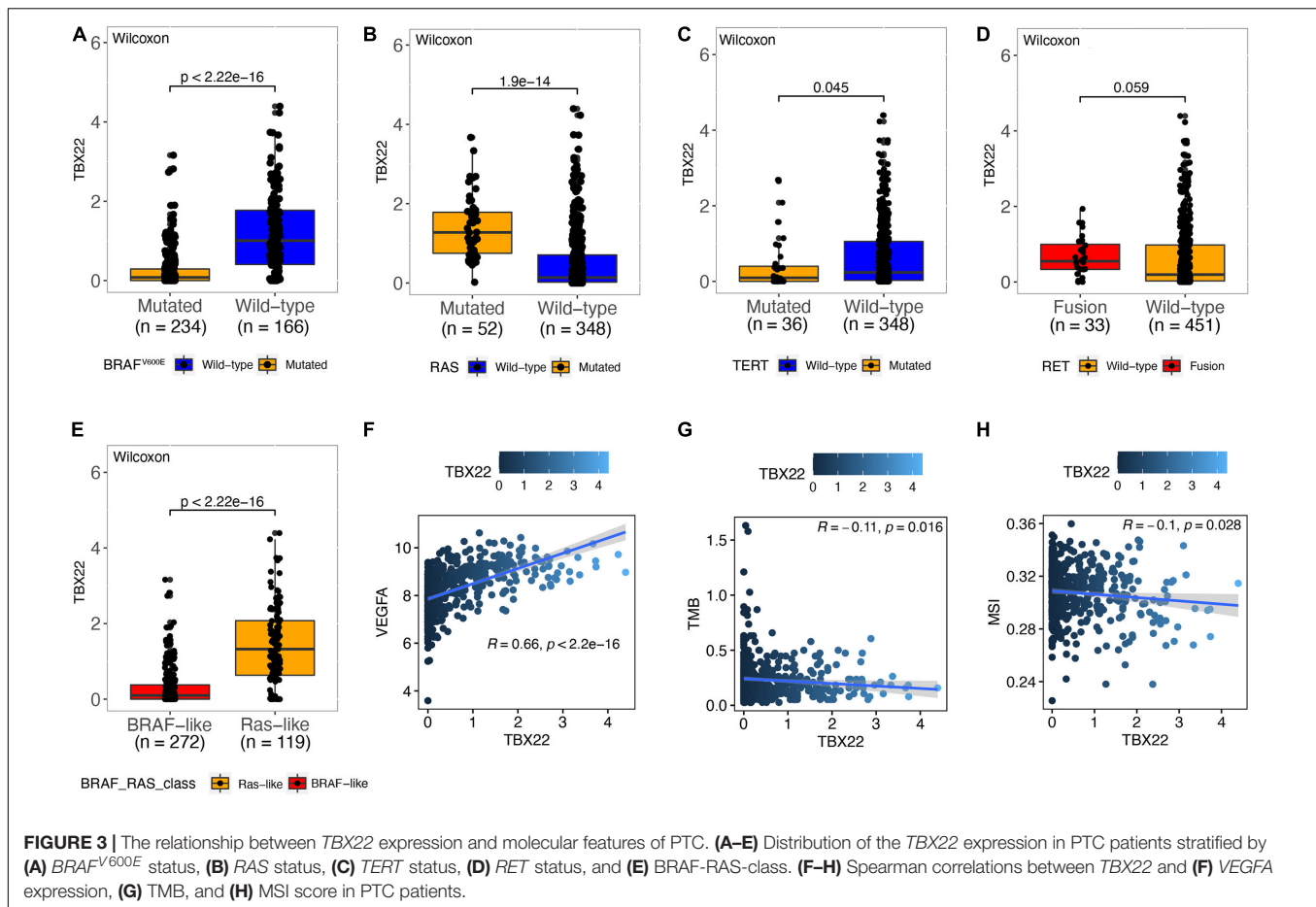
We had found that *TBX22* was associated with T stage and disease stage in PTC patients (Figures 2A,D,F). To determine the function of *TBX22* in PTC tumorigenesis and progression, we knocked down *TBX22* in PTC cell lines using *TBX22*-targeting siRNA (si-*TBX22*). In contrast, we performed gain-of-function studies and generated control (VECTOR) and *TBX22*-overexpressing (*TBX22*-OE) PTC cell lines. The silenced (Figure 9B) and overexpressed (Figure 9C) efficiency of *TBX22* were highly effective at the mRNA level evaluated by qRT-PCR. Remarkably, si-*TBX22* cells showed increased cell proliferation *in vitro* compared with si-NC cells (Figure 9D). On the other hand, *TBX22*-OE cells showed decreased cell proliferation *in vitro* compared with VECTOR cells (Figure 9E). In further colony formation assays, the si-*TBX22* cells also showed increased colonies compared with si-NC cells, whereas *TBX22*-OE had decreased colonies compared with VECTOR cells (Figure 9F).

We also had found that the expression of *TBX22* was associated with LNM and ETE in PTC patients (Figures 2B,C,G). To evaluate the impact of dysregulated *TBX22* on metastasis, we performed the assays of cell migration and invasion. si-*TBX22* cells effectively increased migratory ability compared with those in the si-NC group, whereas *TBX22*-OE cells attenuated migratory ability compared with those in the VECTOR group (Figure 10A). Similar results were observed in invasion assays

(Figure 10B). These data showed that *TBX22* might regulate the proliferation, migration, and invasion capacities of the PTC cells.

DISCUSSION

With the treatment of surgery and hormone replacement treatment, most PTC patients have a favorable prognosis. However, radiotherapy and chemotherapy are the only options for the treatment of undifferentiated, recurrent, and metastatic disease, with a median survival of less than 6 months (Mould et al., 2017; Tirrò et al., 2019). Na and Choi (2018) illustrated the close association between immune TME and immunotherapeutic implications in PTC. Thus, it is necessary to reveal the effective molecular mechanism and identify immune-related biomarkers of PTC to guide a more optimized treatment strategy. Recently, accumulating studies show that certain T-box genes also play an important role in cancer progression. Upregulated *TBX2* and *TBX3* promoted tumorigenesis and progression of different types of cancer (Durbin et al., 2018; Crawford et al., 2019; Krstic et al., 2019). In contrast, a recent study revealed that *TBX1* functions as a tumor suppressor in PTC (Wang et al., 2019). As a member of the T-box transcription factor gene family, *TBX22* participated in the development of non-syndromic cleft palate and was reported to be associated with the risk of hypodontia (Braybrook et al., 2001; Kantaputra et al., 2011). To the best of our knowledge, this



is the first research to provide new insights into dissecting the clinical value and potential biological roles of *TBX22* in PTC.

In the present study, we demonstrated that *TBX22* was significantly downregulated in PTC tissues compared with normal thyroid tissues in four public datasets, which contained more than 650 PTC patients. We then examined the *TBX22* mRNA level by our own RT-qPCR profiles as a validated cohort, including 79 matched PTC and adjacent normal tissues. PTC patients with high tumor stage or poor differentiation still have a certain rate of metastasis and mortality with the worse outcomes (Farahati et al., 2004). We also found that *TBX22* expression was negatively associated with advanced clinicopathological characteristics, including larger tumor size, LNM, higher disease stage, and extrathyroidal extension. It reflected that *TBX22* might be associated with the progression of PTC through TCGA analysis. As a validation, we found that *TBX22* was also associated with tumor size and LNM in our local cohort. Using the ROC analysis, *TBX22* level can perfectly predict PTC and normal thyroid tissue types in the four publicly available datasets and our local cohort (all AUC > 0.91). Besides, *TBX22* can also predict T stage and LNM status in the TCGA and local cohorts. All these results indicate that *TBX22* is a potential biomarker in PTC.

In addition to the traditional clinicopathological risk factors, specific molecular profiles (e.g., *BRAF*, *TERT*, and *RET*) may be

used to predict the risk of extrathyroidal extension and lymph node metastases (Xing et al., 2005; Lee et al., 2007; Kim et al., 2012). The relative simplicity of the PTC genome with dominant mutually exclusive driving events enabled previous researches to clearly dissect the fundamental difference in genomic, epigenomic, and proteomic profiles between BVL and RL. In a previous multivariate analysis, the only clinicopathologically significant predictor of persistent disease after 5 years of follow-up was the presence of mutated *BRAF*^{V600E} (Elisei et al., 2012). We observed that the *TBX22* expression is much lower in *BRAF*^{V600E} mutated, *RAS* wild-type, and BVL phenotypes. *TBX22* can predict *BRAF*^{V600E} mutated status in the TCGA and local cohorts using ROC curves. *TERT* mutation had a significantly higher prevalence in aggressive thyroid cancer and served as an independent predictor of persistent disease and mortality for differentiated thyroid cancer. *RET* fusions commonly had BVL phenotype and upregulated MAPK activity. In this study, we found that *TBX22* expression was significantly lower in *TERT* mutation and *RET* wild-type groups. VEGF is a potent stimulator of endothelial cell proliferation, which may help predict the presence of metastases. In a retrospective study of 19 patients with PTC, Klein et al. (2001) had shown that a high level of VEGF correlated with a high risk of metastatic disease. RNA-seq profile from the database showed that *TBX22*

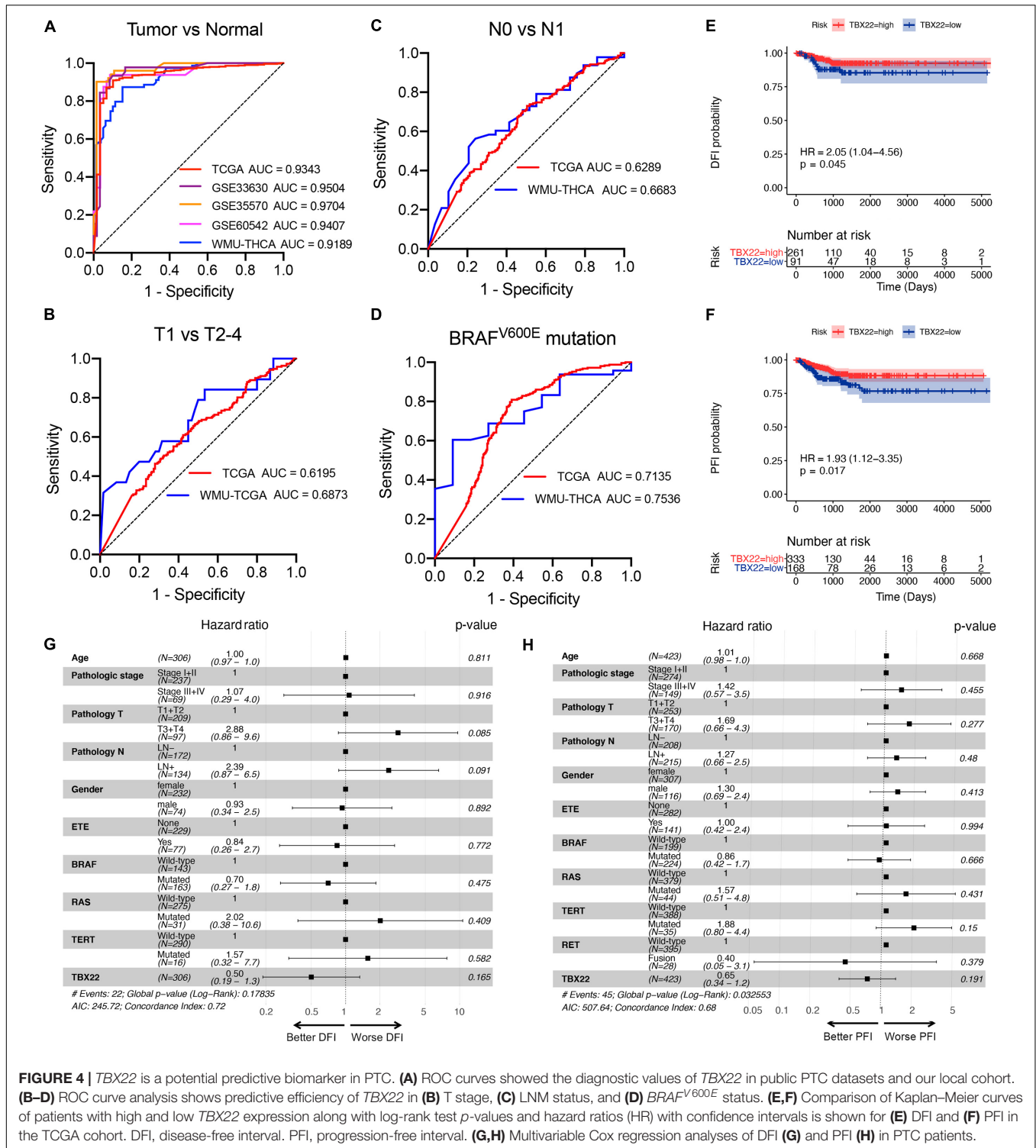


FIGURE 4 | *TBX22* is a potential predictive biomarker in PTC. **(A)** ROC curves showed the diagnostic values of *TBX22* in public PTC datasets and our local cohort. **(B–D)** ROC curve analysis shows predictive efficiency of *TBX22* in **(B)** T stage, **(C)** LNM status, and **(D)** *BRAF*^{V600E} status. **(E,F)** Comparison of Kaplan–Meier curves of patients with high and low *TBX22* expression along with log-rank test *p*-values and hazard ratios (HR) with confidence intervals is shown for **(E)** DFI and **(F)** PFI in the TCGA cohort. DFI, disease-free interval. PFI, progression-free interval. **(G,H)** Multivariable Cox regression analyses of DFI **(G)** and PFI **(H)** in PTC patients.

had a strong positive correlation to VEGF expression. TMB is a novel emerging indicator of immunotherapy and reflects the total mutation index of tumor samples (Chalmers et al., 2017). Tumors with a higher mutation burden are hypothesized to have more opportunities to produce neoantigens that can be recognized by the immune system (Chan et al., 2019). MSI has been found

in many diverse cancer types, including colorectal, endometrial, gastric, prostate, and thyroid cancer (Hause et al., 2016; Genutis et al., 2019). Previous studies showed that MSI-high tumors tend to be poorly differentiated and have an expansile growth pattern, histological heterogeneity, and increased tumor-infiltrating lymphocytes (Zheng et al., 2020). Interestingly, we

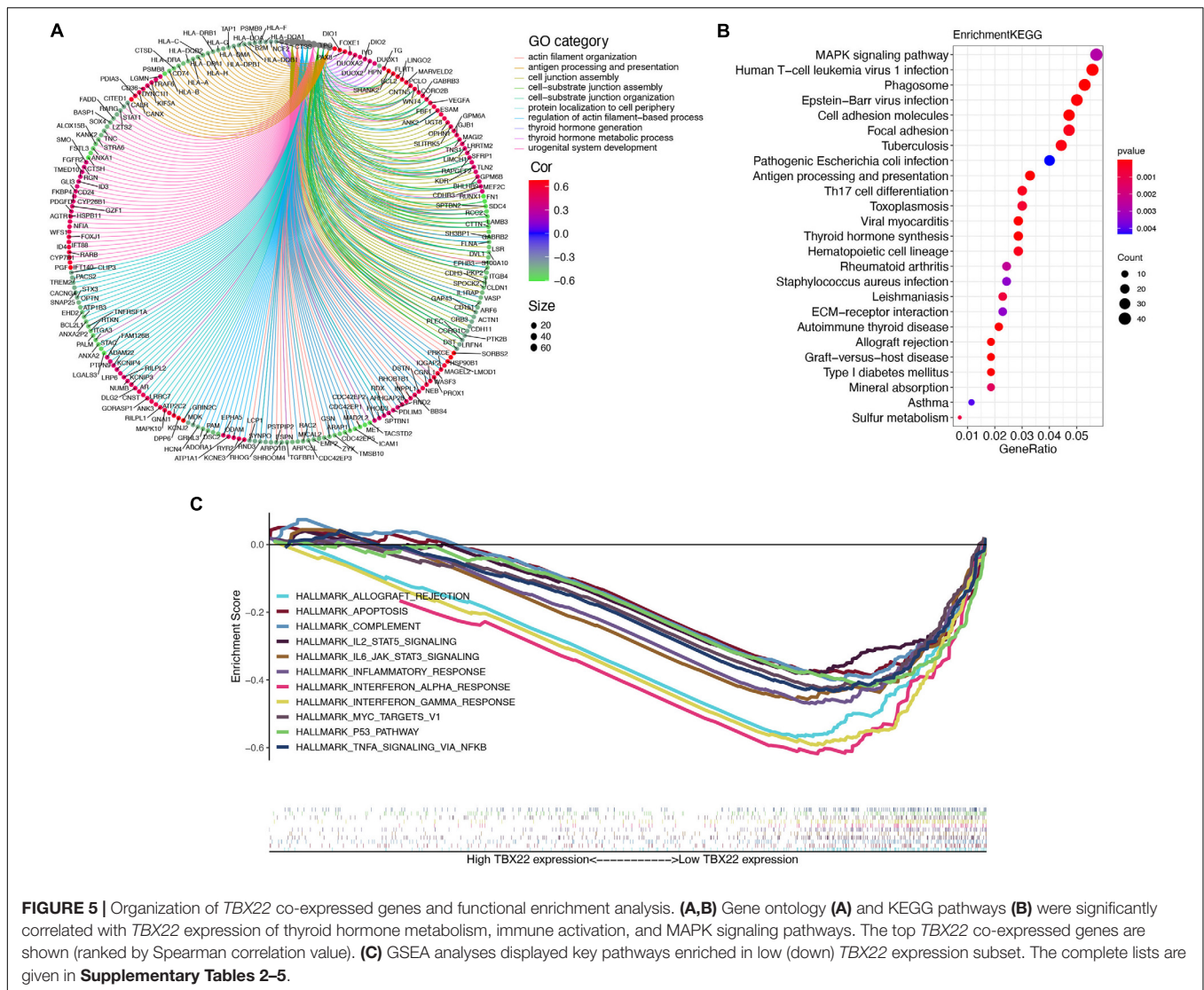


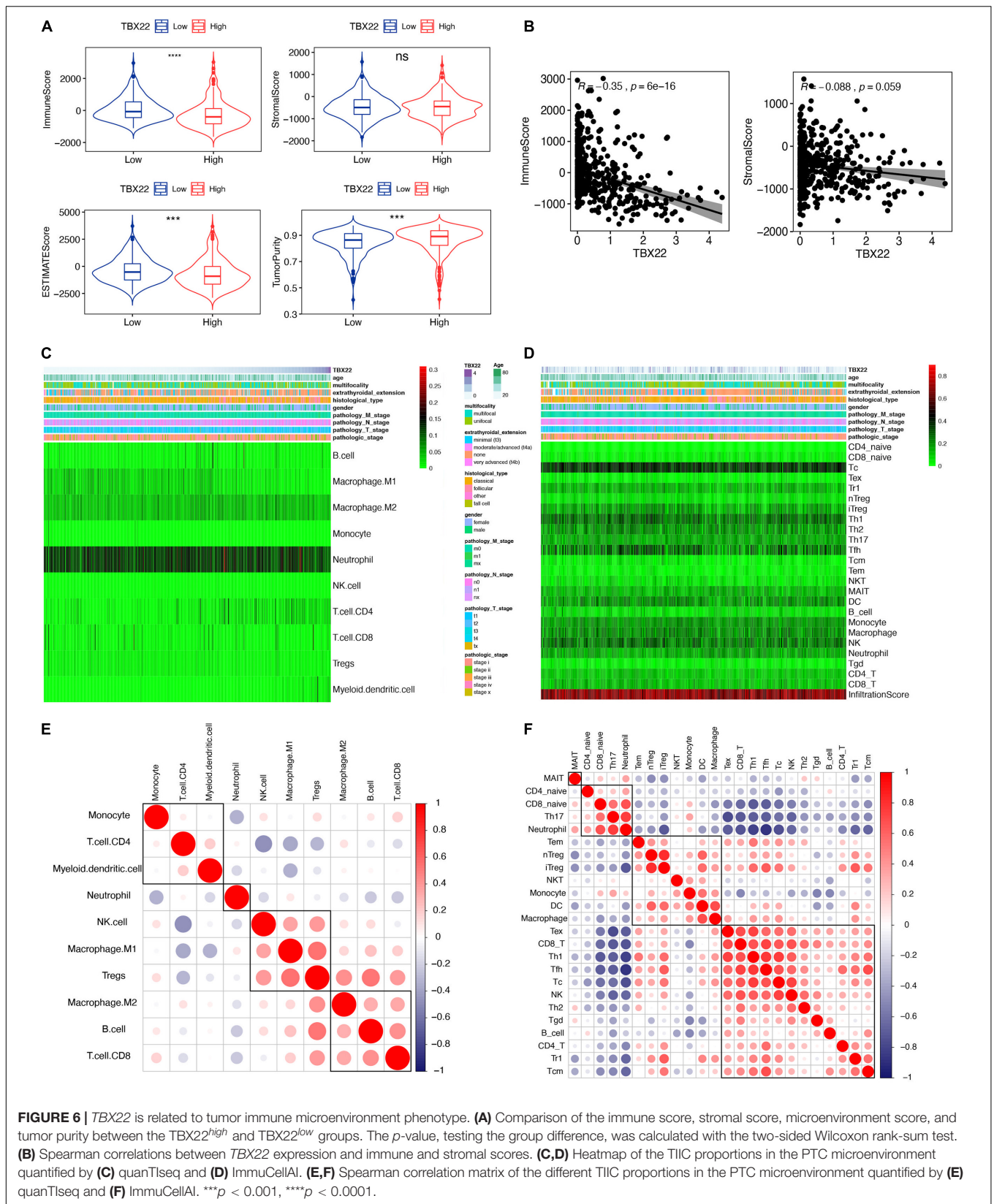
FIGURE 5 | Organization of *TBX22* co-expressed genes and functional enrichment analysis. **(A,B)** Gene ontology **(A)** and KEGG pathways **(B)** were significantly correlated with *TBX22* expression of thyroid hormone metabolism, immune activation, and MAPK signaling pathways. The top *TBX22* co-expressed genes are shown (ranked by Spearman correlation value). **(C)** GSEA analyses displayed key pathways enriched in low (down) *TBX22* expression subset. The complete lists are given in **Supplementary Tables 2–5**.

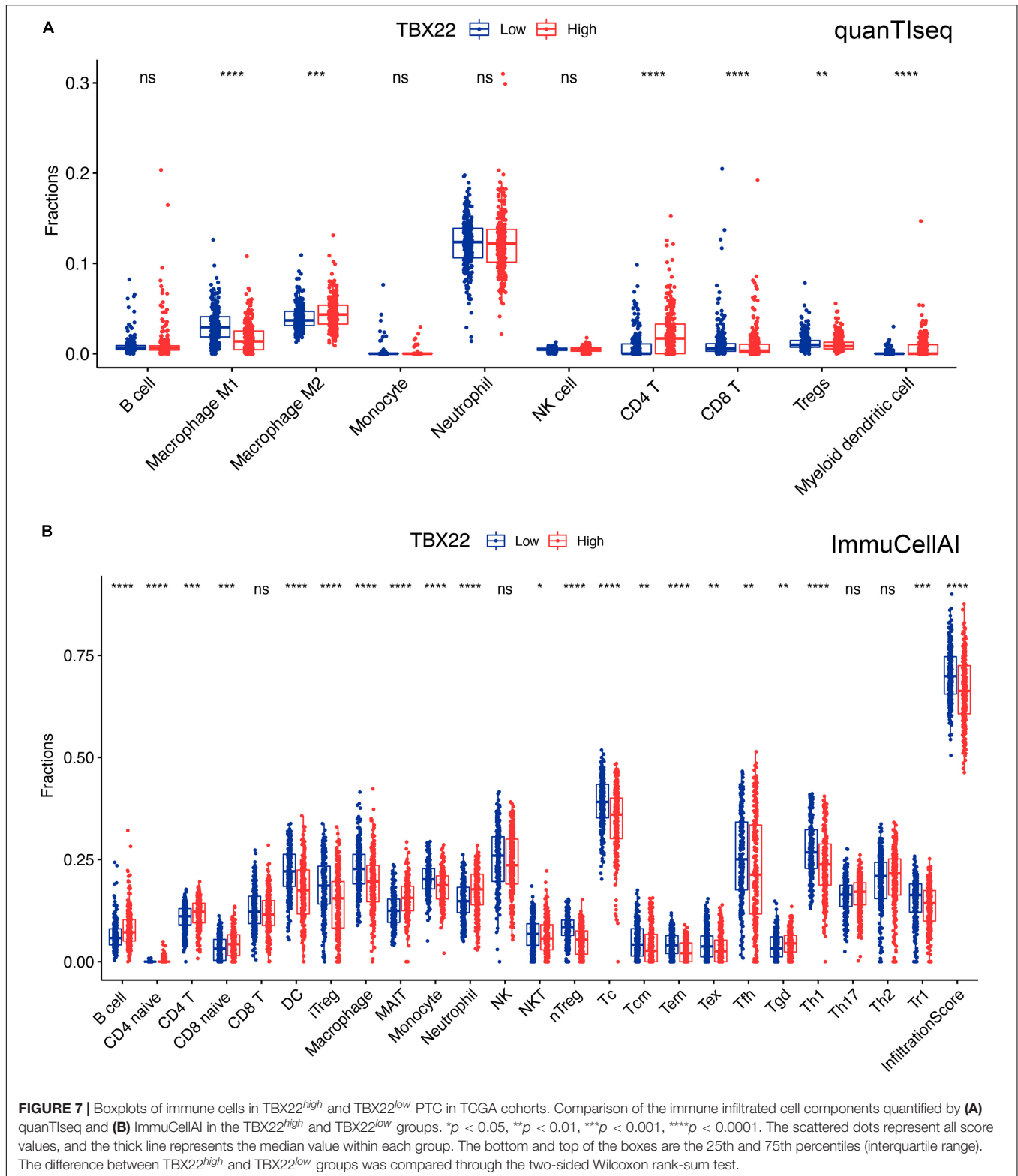
observed a weak correlation between *TBX22* and the status of TMB and MSI in PTC samples. These features are well-known molecular characteristics that affect the prognosis of patients. However, although a number of molecular characteristics were identified to be associated with *TBX22* expression, we found that *TBX22* is not an independent prognostic biomarker in PTC. This may be due to the good prognosis of most PTC patients, leading to a small incidence of DFI and PFI events. These lines of evidence imply that *TBX22* may participate in the regulation of PTC tumorigenesis and progression.

To functionally interpret *TBX22* in the PTC, we investigated possible mechanisms by which *TBX22* affects PTC outcomes from transcriptomic aspects. Co-expressed genes usually act synergistically in biological processes under strict regulatory control, thus having an advantage in adaptive evolution (Niehrs and Pollet, 1999). *TBX22*^{low} status was associated with advanced clinical, pathological, and molecular features. *TBX22* expression was also associated with the enrichment of gene sets related to

the MAPK pathway and thyroid hormone metabolism. More importantly, other than cancer signaling pathways, immune processes such as IL-2 and IL-6 signaling pathways, INF- α and INF- γ response, and complement activity were dominantly associated with *TBX22*^{low} status (14 terms were significant GSEA results, 13 were immune- or cancer-related processes). A deeper analysis of the complexity within TME may promote identifying patient populations for neoadjuvant treatment targets (Lin et al., 2019). Here, we explored the relationship between TME score with *TBX22* expression based on two different computational algorithms. Our study identified that *TBX22* expression was negatively associated with immune scores but not significant with stromal scores. Based on the functional enrichment analysis of *TBX22* and its correlation with TIME above, we hypothesized that *TBX22* was associated with immune cell component in the PTC microenvironment.

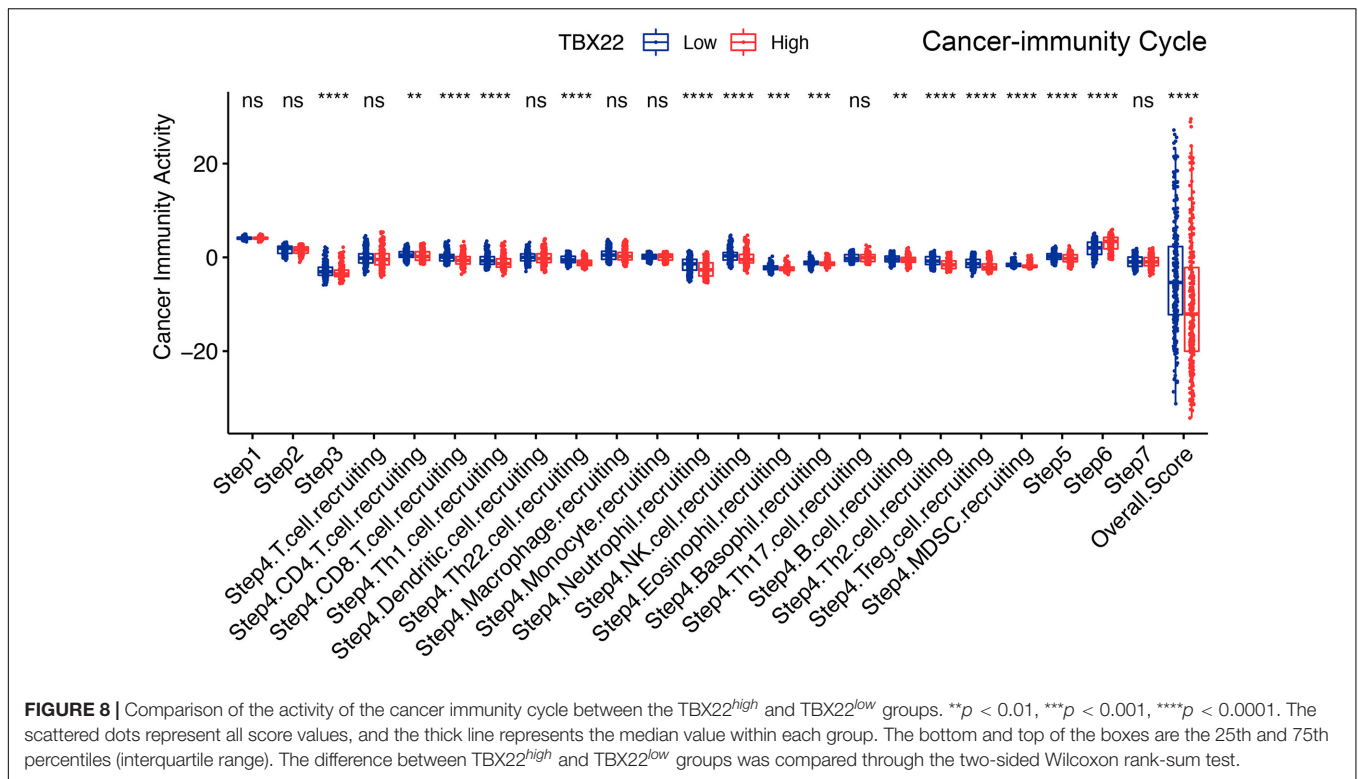
The deconvolution technique has been proven to be useful in the decomposition of heterogeneous cellular admixture of





TME (Gentles et al., 2015; Orhan et al., 2020). As there is no gold standard for inferring immune infiltrate from the RNA-seq profile, we chose ssGSEA-based ImmuCellAI and

deconvolution-based quanTseq algorithms in inferring the composition of TIICs. Cunha et al. (2012, 2015) demonstrated that a higher CD8⁺ T-cell infiltration level was related to better

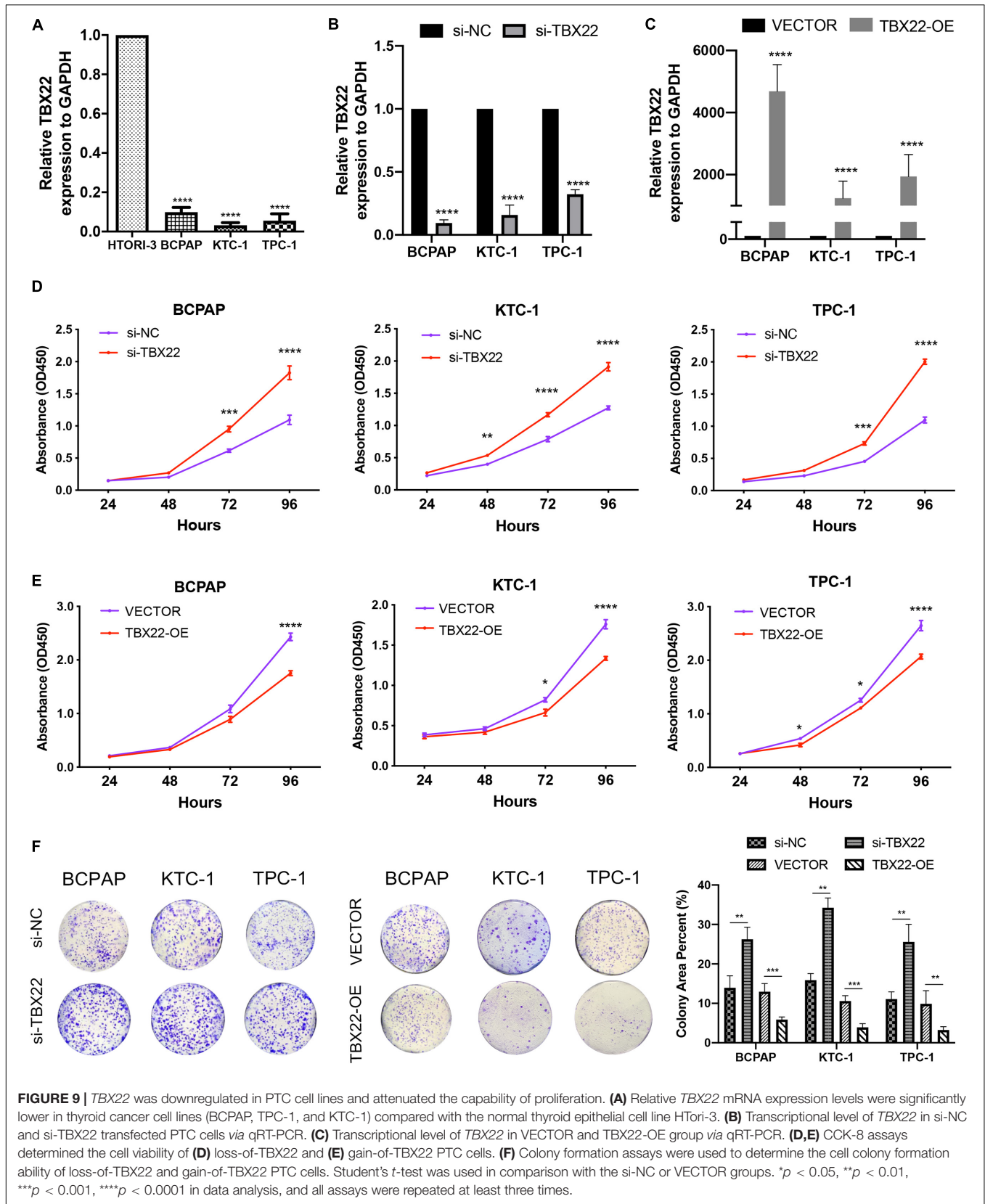


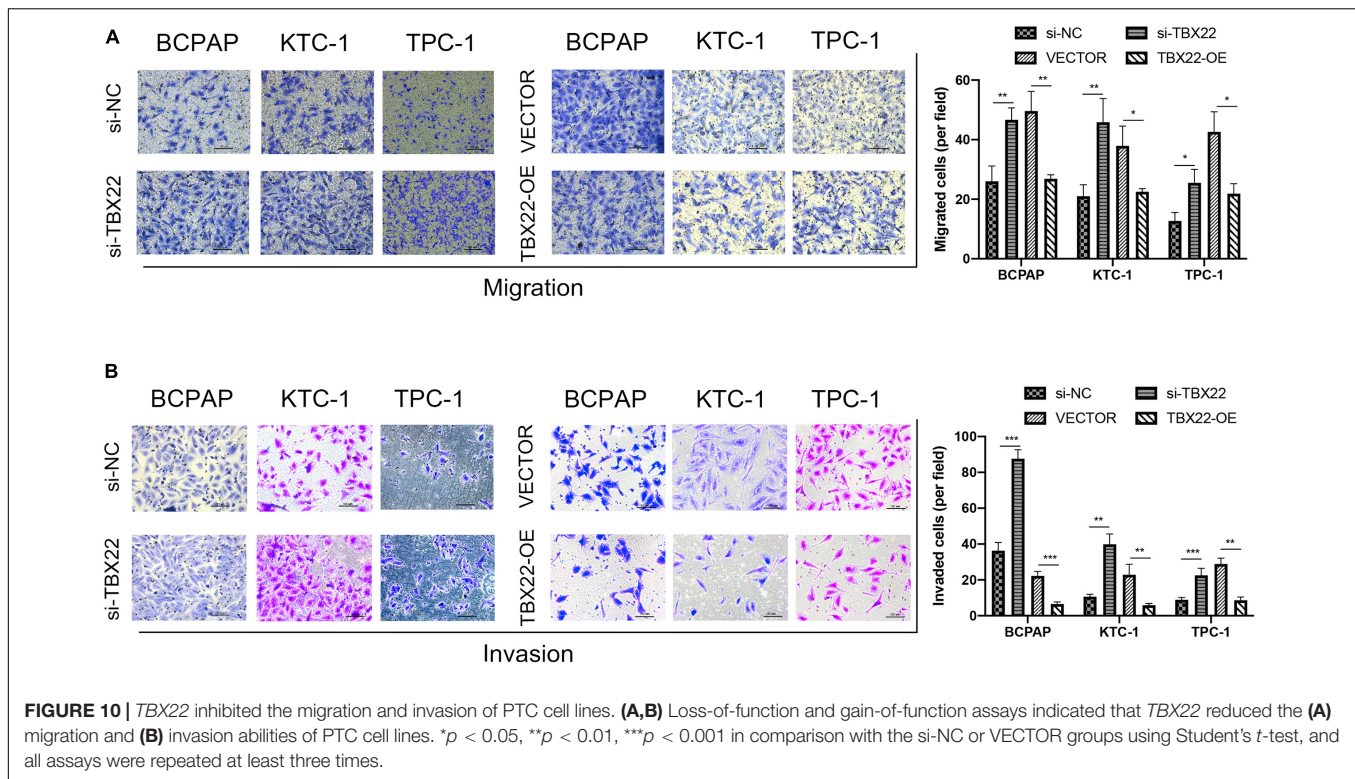
disease-free survival rate and increased risk of relapse of PTC. A previous study indicated that tumors with high $CD8^+$ T cells are more likely to respond to immunotherapy than the low $CD8^+$ T-cell tumors (Farhood et al., 2019). Furthermore, an increase in anticancer $CD8^+$ T, Tfh, and Th1 cells and M1 macrophages and a decrease in procancer M2 macrophages were associated with $TBX22^{low}$ in PTC. In addition, we also found that the distribution of $CD4^+$ T cells was accordantly lower in the $TBX22^{low}$ group. We noticed that the infiltration levels of procancerous $CD4^+$ T and Tregs cells in $TBX22^{low}$ samples were higher, and procancerous Th2 cells had an elevated activity score in cancer immune cycle in $TBX22^{low}$ samples, which may lead to the cancer-promoting phenotype corresponding to $TBX22^{low}$ status (Hadrup et al., 2013; Tanaka and Sakaguchi, 2017; Wu et al., 2017).

The main goal of immunotherapy is to trigger the cancer immunity cycle without damaging normal cells. Based on this consideration, many current immunotherapeutic agents like CTLA-4 and PD-L1 inhibitors target steps in the cancer immunity cycle (Chen and Mellman, 2017). Patients who have lower $TBX22$ expression showed higher anticancer immunity scores in different steps of the cancer immunity cycle. We found that lower $TBX22$ expression led to more recruitment of anticancer $CD8^+$ T cells, Th1, Tregs, and NK cells, which conform to the results of TIME alteration. Besides, we found that $TBX22^{low}$ did appear to be associated with a favorable TIME in PTC. These results support that $TBX22$ may manipulate the activity of the cancer immunity cycle.

TIICs in the TME may affect tumor cell proliferation, metastasis, and therapy resistance (Gocheva et al., 2010; Joyce and Fearon, 2015). However, there has been no experimental study to elucidate the functional effects of $TBX22$ dysregulation in PTC models. Transfection efficiency and background expression of the $TBX22$ in different PTC cell lines were considered. The significance of $TBX22$ is demonstrated through loss-of-function, which increased the proliferation, migration, and invasion ability of PTC cells. Conversely, the gain-of-function addition of $TBX22$ to PTC cells demonstrated attenuated proliferation, migration, and invasion. Together, these findings suggest that $TBX22$ exerts a considerable tumor-suppressor effect in PTC.

The current study has several limitations. Firstly, more local tumor samples are needed to verify the relationship between $TBX22$ and the clinical characteristics and confirm its predictive performance as a biomarker in PTC. Secondly, most of the existing TME computational methods are limited to only a single omics layer, which may not be enough to detect particular biological processes. It is necessary to quantify the particular biological processes and TME heterogeneity by multidimensional omics data. Thirdly, our research revealed a markedly close interaction between $TBX22$ and anticancer immunity, as well as tumorigenesis and progression in PTC. However, the underlying $TBX22$ -related mechanisms in PTC are yet to be fully elucidated. Constructing *in vivo* models to explore the potential biological mechanisms of $TBX22$ is the direction of future research. Lastly, the potential cross talk between the $BRAF^{V600E}$ mutation and TIME alteration in $TBX22$ -induced PTC progression requires further exploration.





CONCLUSION

The involvement of *TBX22* in PTC appears to be highly complex. Our study is the first to identify the expression level and the relationship with the clinicopathological and molecular features, tumor-infiltrating, cancer immunity cycle, and functional effects of *TBX22* in PTC. The present study sheds light to conduct further *TBX22*-associated research to assess its efficacy and receptiveness in PTC treatment.

DATA AVAILABILITY STATEMENT

The original contributions generated for this study are included in the article/**Supplementary Material**, further inquiries can be directed to the corresponding author/s.

ETHICS STATEMENT

All research protocols have been approved and implemented through the ethical standards of the institutional review board of the First Affiliated Hospital of Wenzhou Medical University (Approval No. 2012-57). The patients/participants provided their written informed consent to participate in this study.

AUTHOR CONTRIBUTIONS

XD and JS contributed to study design, bioinformatic analysis, and manuscript draft. JH and CZ contributed to sample

preparation and molecular biology experiments. XZ and HL contributed to the revision of the manuscript. All authors read and approved the final manuscript.

FUNDING

This study was supported by the Major Science and Technology Projects of Zhejiang Province (2015C03052).

ACKNOWLEDGMENTS

The authors would like to thank the investigators and staff who contributed to this study.

SUPPLEMENTARY MATERIAL

The Supplementary Material for this article can be found online at: <https://www.frontiersin.org/articles/10.3389/fcell.2020.590898/full#supplementary-material>

Supplementary Table 1 | Univariate Cox regression of clinical and pathological factors in PTC patients.

Supplementary Table 2 | *TBX22* co-expressed genes detailed results.

Supplementary Table 3 | GO enrichment detailed results.

Supplementary Table 4 | KEGG enrichment detailed results.

Supplementary Table 5 | GSEA enrichment detailed results.

REFERENCES

- Agrawal, N., Akbani, R., Aksoy, B. A., Ally, A., Arachchi, H., Asa, S. L., et al. (2014). Integrated genomic characterization of papillary thyroid carcinoma. *Cell* 159, 676–690.
- Asioli, S., Erickson, L. A., Sebo, T. J., Zhang, J., Jin, L., Thompson, G. B., et al. (2010). Papillary thyroid carcinoma with prominent hobnail features: a new aggressive variant of moderately differentiated papillary carcinoma. A clinicopathologic, immunohistochemical, and molecular study of eight cases. *Am. J. Surg. Pathol.* 34, 44–52. doi: 10.1097/pas.0b013e3181c46677
- Bonneville, R., Krook, M. A., Kautto, E. A., Miya, J., Wing, M. R., Chen, H.-Z., et al. (2017). Landscape of microsatellite instability across 39 cancer types. *JCO Precis Oncol.* 2017:PO.17.00073. doi: 10.1200/PO.17.00073
- Braybrook, C., Doudney, K., Marçano, A. C. B., Arnason, A., Björnsson, A., Patton, M. A., et al. (2001). The T-box transcription factor gene TBX22 is mutated in X-linked cleft palate and ankyloglossia. *Nat. Genet.* 29, 179–183. doi: 10.1038/ng730
- Cancer Genome Atlas Research Network (2014). Integrated genomic characterization of papillary thyroid carcinoma. *Cell* 159, 676–690. doi: 10.1016/j.cell.2014.09.050
- Chalmers, Z. R., Connelly, C. F., Fabrizio, D., Gay, L., Ali, S. M., Ennis, R., et al. (2017). Analysis of 100,000 human cancer genomes reveals the landscape of tumor mutational burden. *Genome Med.* 9:34.
- Chan, T. A., Yarchoan, M., Jaffee, E., Swanton, C., Quezada, S. A., Stenzinger, A., et al. (2019). Development of tumor mutation burden as an immunotherapy biomarker: utility for the oncology clinic. *Ann. Oncol.* 30, 44–56. doi: 10.1093/annonc/mdy495
- Chen, D. S., and Mellman, I. (2013). Oncology meets immunology: the cancer-immunity cycle. *Immunity* 39, 1–10. doi: 10.1016/j.immuni.2013.07.012
- Chen, D. S., and Mellman, I. (2017). Elements of cancer immunity and the cancer-immune set point. *Nature* 541, 321–330. doi: 10.1038/nature21349
- Cheng, H. S., Lee, J. X. T., Wahli, W., and Tan, N. S. (2019). Exploiting vulnerabilities of cancer by targeting nuclear receptors of stromal cells in tumor microenvironment. *Mol. Cancer* 18:51.
- Crawford, N., McIntyre, A., McCormick, A., D'Costa, Z., Buckley, N., and Mullan, P. (2019). TBX2 interacts with heterochromatin protein 1 to recruit a novel repression complex to EGFR1-targeted promoters to drive the proliferation of breast cancer cells. *Oncogene* 38, 5971–5986. doi: 10.1038/s41388-019-0853-z
- Cunha, L. L., Marcello, M. A., Nonogaki, S., Morari, E. C., Soares, F. A., Vassallo, J., et al. (2015). CD 8+ tumour-infiltrating lymphocytes and COX2 expression may predict relapse in differentiated thyroid cancer. *Clin. Endocrinol.* 83, 246–253. doi: 10.1111/cen.12586
- Cunha, L. L., Morari, E. C., Guihen, A. C., Razolli, D., Gerhard, R., Nonogaki, S., et al. (2012). Infiltration of a mixture of immune cells may be related to good prognosis in patients with differentiated thyroid carcinoma. *Clin. Endocrinol.* 77, 918–925. doi: 10.1111/j.1365-2265.2012.04482.x
- Deschoolmeester, V., Baay, M., Van Marck, E., Weyler, J., Vermeulen, P., Lardon, F., et al. (2010). Tumor infiltrating lymphocytes: an intriguing player in the survival of colorectal cancer patients. *BMC Immunol.* 11:19. doi: 10.1186/1471-2172-11-19
- Dom, G., Tarabichi, M., Unger, K., Thomas, G., Oczko-Wojciechowska, M., Bogdanova, T., et al. (2012). A gene expression signature distinguishes normal tissues of sporadic and radiation-induced papillary thyroid carcinomas. *Br. J. Cancer* 107, 994–1000. doi: 10.1038/bjc.2012.302
- Dong, X., Gu, D.-N., Wang, O., and Ye, Z. (2020a). LAGE3 correlates with tumorigenic immune infiltrates in the clear cell renal cell carcinoma microenvironment. *Int. Immunopharmacol.* 87:106793. doi: 10.1016/j.intimp.2020.106793
- Dong, X., Lv, S., Zhang, X., and Hao, R. (2020b). Upregulation of LAGE3 correlates with prognosis and immune infiltrates in colorectal cancer: a bioinformatic analysis. *Int. Immunopharmacol.* 85:106599. doi: 10.1016/j.intimp.2020.106599
- Durbin, A. D., Zimmerman, M. W., Dharia, N. V., Abraham, B. J., Iniguez, A. B., Weichert-Leahey, N., et al. (2018). Selective gene dependencies in MYCN-amplified neuroblastoma include the core transcriptional regulatory circuitry. *Nat. Genet.* 50, 1240–1246. doi: 10.1038/s41588-018-0191-z
- Elisei, R., Viola, D., Torregrossa, L., Giannini, R., Romei, C., Ugolini, C., et al. (2012). The BRAF V600E mutation is an independent, poor prognostic factor for the outcome of patients with low-risk intrathyroid papillary thyroid carcinoma: single-institution results from a large cohort study. *J. Clin. Endocrinol. Metabol.* 97, 4390–4398. doi: 10.1210/jc.2012-1775
- Emens, L. A., Ascierto, P. A., Darcy, P. K., Demaria, S., Eggermont, A. M., Redmond, W. L., et al. (2017). Cancer immunotherapy: opportunities and challenges in the rapidly evolving clinical landscape. *Eur. J. Cancer* 81, 116–129. doi: 10.1016/j.ejca.2017.01.035
- Farahati, J., Geling, M., Mäder, U., Mörtl, M., Luster, M., Müller, J. G., et al. (2004). Changing trends of incidence and prognosis of thyroid carcinoma in lower Franconia, Germany, from 1981–1995. *Thyroid* 14, 141–147.
- Farhood, B., Najafi, M., and Mortezaee, K. (2019). CD8+ cytotoxic T lymphocytes in cancer immunotherapy: a review. *J. Cell. Physiol.* 234, 8509–8521. doi: 10.1002/jcp.27782
- Finotello, F., Mayer, C., Plattner, C., Laschober, G., Rieder, D., Hackl, H., et al. (2019). Molecular and pharmacological modulators of the tumor immune contexture revealed by deconvolution of RNA-seq data. *Genome Med.* 11:34.
- Gentles, A. J., Newman, A. M., Liu, C. L., Bratman, S. V., Feng, W., Kim, D., et al. (2015). The prognostic landscape of genes and infiltrating immune cells across human cancers. *Nat. Med.* 21, 938–945. doi: 10.1038/nm.3909
- Genutis, L. K., Tomsic, J., Bundschuh, R. A., Brock, P. L., Williams, M. D., Roychowdhury, S., et al. (2019). Microsatellite instability occurs in a subset of follicular thyroid cancers. *Thyroid* 29, 523–529. doi: 10.1089/thy.2018.0655
- Ghossein, R., and Livolsi, V. A. (2008). Papillary thyroid carcinoma tall cell variant. *Thyroid* 18, 1179–1181. doi: 10.1089/thy.2008.0164
- Ghossein, R. A., Leboeuf, R., Patel, K. N., Rivera, M., Katabi, N., Carlson, D. L., et al. (2007). Tall cell variant of papillary thyroid carcinoma without extrathyroid extension: biologic behavior and clinical implications. *Thyroid* 17, 655–661. doi: 10.1089/thy.2007.0061
- Gocheva, V., Wang, H.-W., Gadea, B. B., Shree, T., Hunter, K. E., Garfall, A. L., et al. (2010). IL-4 induces cathepsin protease activity in tumor-associated macrophages to promote cancer growth and invasion. *Genes Dev.* 24, 241–255. doi: 10.1101/gad.1874010
- Guzman, C., Bagga, M., Kaur, A., Westermarck, J., and Abankwa, D. (2014). ColonyArea: an ImageJ plugin to automatically quantify colony formation in clonogenic assays. *PLoS One* 9:e92444. doi: 10.1371/journal.pone.0092444
- Hadrup, S., Donia, M., and Thor Straten, P. (2013). Effector CD4 and CD8 T cells and their role in the tumor microenvironment. *Cancer Microenviron.* 6, 123–133. doi: 10.1007/s12307-012-0127-6
- Handkiewicz-Junak, D., Swierniak, M., Rusinek, D., Oczko-Wojciechowska, M., Dom, G., Maenhaut, C., et al. (2016). Gene signature of the post-Chernobyl papillary thyroid cancer. *Eur. J. Nucl. Med. Mol. Imaging* 43, 1267–1277.
- Hause, R. J., Pritchard, C. C., Shendure, J., and Salipante, S. J. (2016). Classification and characterization of microsatellite instability across 18 cancer types. *Nat. Med.* 22, 1342–1350. doi: 10.1038/nm.4191
- James, B. C., Mitchell, J. M., Jeon, H. D., Vasilottos, N., Grogan, R. H., and Aschebrook-Kilfoy, B. (2018). An update in international trends in incidence rates of thyroid cancer, 1973–2007. *Cancer Causes Control* 29, 465–473. doi: 10.1007/s10552-018-1023-2
- Jia, Z., Liu, Y., Guan, N., Bo, X., Luo, Z., and Barnes, M. R. (2016). Cogena, a novel tool for co-expressed gene-set enrichment analysis, applied to drug repositioning and drug mode of action discovery. *BMC Genomics* 17:414. doi: 10.1186/s12864-016-2737-8
- Johnson, T. L., Lloyd, R. V., Thompson, N. W., Beierwaltes, W. H., and Sisson, J. C. (1988). Prognostic implications of the tall cell variant of papillary thyroid carcinoma. *Am. J. Surg. Pathol.* 12, 22–27.
- Joyce, J. A., and Fearon, D. T. (2015). T cell exclusion, immune privilege, and the tumor microenvironment. *Science* 348, 74–80. doi: 10.1126/science.aaa6204
- Kantaputra, P., Paramee, M., Kaewkhampa, A., Hoshino, A., Lees, M., McEntagart, M., et al. (2011). Cleft lip with cleft palate, ankyloglossia, and hypodontia are associated with TBX22 mutations. *J. Dent. Res.* 90, 450–455. doi: 10.1177/0022034510391052
- Kim, T. H., Park, Y. J., Lim, J. A., Ahn, H. Y., Lee, E. K., Lee, Y. J., et al. (2012). The association of the BRAFV600E mutation with prognostic factors and poor clinical outcome in papillary thyroid cancer: a meta-analysis. *Cancer* 118, 1764–1773. doi: 10.1002/cncr.26500

- Klein, M., Vignaud, J.-M., Hennequin, V., Toussaint, B., Bresler, L., Plenat, F., et al. (2001). Increased expression of the vascular endothelial growth factor is a pejorative prognosis marker in papillary thyroid carcinoma. *J. Clin. Endocrinol. Metab.* 86, 656–658. doi: 10.1210/jcem.86.2.7226
- Krstic, M., Kolendowski, B., Cecchini, M. J., Postenka, C. O., Hassan, H. M., Andrews, J., et al. (2019). TBX3 promotes progression of pre-invasive breast cancer cells by inducing EMT and directly up-regulating SLUG. *J. Pathol.* 248, 191–203. doi: 10.1002/path.5245
- Landa, I., Ganly, I., Chan, T. A., Mitsutake, N., Matsuse, M., Ibrahimspasic, T., et al. (2013). Frequent somatic TERT promoter mutations in thyroid cancer: higher prevalence in advanced forms of the disease. *J. Clin. Endocrinol. Metab.* 98, E1562–E1566.
- Landa, I., Ibrahimspasic, T., Boucai, L., Sinha, R., Knauf, J. A., Shah, R. H., et al. (2016). Genomic and transcriptomic hallmarks of poorly differentiated and anaplastic thyroid cancers. *J. Clin. Invest.* 126, 1052–1066. doi: 10.1172/jci85271
- Landa, I., Pozdeyev, N., Korch, C., Marlow, L. A., Smallridge, R. C., Copland, J. A., et al. (2019). Comprehensive genetic characterization of human thyroid cancer cell lines: a validated panel for preclinical studies. *Clin. Cancer Res.* 25, 3141–3151. doi: 10.1158/1078-0432.ccr-18-2953
- Lee, J. H., Lee, E. S., and Kim, Y. S. (2007). Clinicopathologic significance of BRAF V600E mutation in papillary carcinomas of the thyroid: a meta-analysis. *Cancer* 110, 38–46. doi: 10.1002/ncr.22754
- Lin, P., Guo Y-n, Shi, L., Li, X.-J., Yang, H., He, Y., et al. (2019). Development of a prognostic index based on an immunogenomic landscape analysis of papillary thyroid cancer. *Aging* 11:480. doi: 10.18632/aging.101754
- Liu, J., Lichtenberg, T., Hoadley, K. A., Poisson, L. M., Lazar, A. J., Cherniack, A. D., et al. (2018). An integrated TCGA pan-cancer clinical data resource to drive high-quality survival outcome analytics. *Cell* 173, 400.e11–416.e11.
- Mao, Y., Keller, E. T., Garfield, D. H., Shen, K., and Wang, J. (2013). Stromal cells in tumor microenvironment and breast cancer. *Cancer Metastasis Rev.* 32, 303–315.
- Meireles, A. M., Preto, A., Rocha, A. S., Rebocho, A. P., Máximo, V., Pereira-Castro, I., et al. (2007). Molecular and genotypic characterization of human thyroid follicular cell carcinoma-derived cell lines. *Thyroid* 17, 707–715. doi: 10.1089/thy.2007.0097
- Miao, Y. R., Zhang, Q., Lei, Q., Luo, M., Xie, G. Y., Wang, H., et al. (2020). ImmuCellAI: a unique method for comprehensive T-cell subsets abundance prediction and its application in cancer immunotherapy. *Adv. Sci.* 7:1902880.
- Miller, S. A., Mohn, S. E., and Weinmann, A. S. (2010). Jmjd3 and UTX play a demethylase-independent role in chromatin remodeling to regulate T-box family member-dependent gene expression. *Mol. Cell* 40, 594–605.
- Mould, R. C., van Vloten, J. P., AuYeung, A. W., Karimi, K., and Bridle, B. W. (2017). Immune responses in the thyroid cancer microenvironment: making immunotherapy a possible mission. *Endocr. Relat. Cancer* 24, T311–T329.
- Na, K. J., and Choi, H. (2018). Immune landscape of papillary thyroid cancer and immunotherapeutic implications. *Endocr. Relat. Cancer* 25, 523–531.
- Niehrs, C., and Pollet, N. (1999). Synexpression groups in eukaryotes. *Nature* 402, 483–487.
- Orhan, A., Vogelsang, R. P., Andersen, M. B., Madsen, M. T., Hölmich, E. R., Raskov, H., et al. (2020). The prognostic value of tumour-infiltrating lymphocytes in pancreatic cancer: a systematic review and meta-analysis. *Eur. J. Cancer* 132, 71–84. doi: 10.1016/j.ejca.2020.03.013
- Papaioannou, V. E. (2014). The T-box gene family: emerging roles in development, stem cells and cancer. *Development* 141, 3819–3833.
- Randolph, G. W., Duh, Q.-Y., Heller, K. S., LiVolsi, V. A., Mandel, S. J., Steward, D. L., et al. (2012). The prognostic significance of nodal metastases from papillary thyroid carcinoma can be stratified based on the size and number of metastatic lymph nodes, as well as the presence of extranodal extension. *Thyroid* 22, 1144–1152.
- Sebé-Pedros, A., Ariza-Cosano, A., Weirauch, M. T., Leininger, S., Yang, A., Torruella, G., et al. (2013). Early evolution of the T-box transcription factor family. *Proc. Natl. Acad. Sci. U.S.A.* 110, 16050–16055.
- Subramanian, A., Tamayo, P., Mootha, V. K., Mukherjee, S., Ebert, B. L., Gillette, M. A., et al. (2005). Gene set enrichment analysis: a knowledge-based approach for interpreting genome-wide expression profiles. *Proc. Natl. Acad. Sci. U.S.A.* 102, 15545–15550.
- Tanaka, A., and Sakaguchi, S. (2017). Regulatory T cells in cancer immunotherapy. *Cell Res.* 27, 109–118.
- Tarabichi, M., Saiselet, M., Trésallet, C., Hoang, C., Larsimont, D., Andry, G., et al. (2015). Revisiting the transcriptional analysis of primary tumours and associated nodal metastases with enhanced biological and statistical controls: application to thyroid cancer. *Br. J. Cancer* 112, 1665–1674. doi: 10.1038/bjc.2014.665
- Tirró, E., Martorana, F., Romano, C., Vitale, S. R., Motta, G., Di Gregorio, S., et al. (2019). Molecular alterations in thyroid cancer: from bench to clinical practice. *Genes* 10:709.
- Wang, N., Li, Y., Wei, J., Pu, J., Liu, R., Yang, Q., et al. (2019). TBX1 functions as a tumor suppressor in thyroid cancer through inhibiting the activities of the PI3K/AKT and MAPK/ERK pathways. *Thyroid* 29, 378–394.
- Wu, Y., Yan, Y., Su, Z., Bie, Q., Chen, X., Barnie, P. A., et al. (2017). Enhanced circulating ILC2s and MDSCs may contribute to ensure maintenance of Th2 predominant in patients with lung cancer. *Mol. Med. Rep.* 15, 4374–4381.
- Xing, M., Westra, W. H., Tufano, R. P., Cohen, Y., Rosenbaum, E., Rhoden, K. J., et al. (2005). BRAF mutation predicts a poorer clinical prognosis for papillary thyroid cancer. *J. Clin. Endocrinol. Metab.* 90, 6373–6379.
- Xu, L., Deng, C., Pang, B., Zhang, X., Liu, W., Liao, G., et al. (2018). TIP: a web server for resolving tumor immunophenotype profiling. *Cancer Res.* 78, 6575–6580. doi: 10.1158/0008-5472.Can-18-0689
- Yoo, S.-K., Lee, S., Kim, S.-J., Jee, H.-G., Kim, B.-A., Cho, H., et al. (2016). Comprehensive analysis of the transcriptional and mutational landscape of follicular and papillary thyroid cancers. *PLoS Genet.* 12:e1006239. doi: 10.1371/journal.pgen.1006239
- Yoshihara, K., Shahmoradgoli, M., Martínez, E., Vegesna, R., Kim, H., Torres-García, W., et al. (2013). Inferring tumour purity and stromal and immune cell admixture from expression data. *Nat. Commun.* 4:2612.
- Yu, K., Ganesan, K., Tan, L. K., Laban, M., Wu, J., Zhao, X. D., et al. (2008). A precisely regulated gene expression cassette potently modulates metastasis and survival in multiple solid cancers. *PLoS Genet.* 4:e1000129. doi: 10.1371/journal.pgen.1000129
- Zheng, K., Wan, H., Zhang, J., Shan, G., Chai, N., Li, D., et al. (2020). A novel NGS-based microsatellite instability (MSI) status classifier with 9 loci for colorectal cancer patients. *J. Transl. Med.* 18:215.

Conflict of Interest: The authors declare that the research was conducted in the absence of any commercial or financial relationships that could be construed as a potential conflict of interest.

Copyright © 2020 Dong, Song, Hu, Zheng, Zhang and Liu. This is an open-access article distributed under the terms of the Creative Commons Attribution License (CC BY). The use, distribution or reproduction in other forums is permitted, provided the original author(s) and the copyright owner(s) are credited and that the original publication in this journal is cited, in accordance with accepted academic practice. No use, distribution or reproduction is permitted which does not comply with these terms.